Strain control of spintronic devices

Egor Savostin[1], Jiawei Duan[1], and Vitaliy Lomakin[1], *Fellow, IEEE*

[1]Center for Memory and Recording Research and Department of Electrical and Computer Engineering, University of California, San Diego, California 92093, USA, vlomakin@ucsd.edu

This work presents a theoretical and numerical study of strain-controlled magnetic and spintronic devices. A finite-element micromagnetic framework is introduced that self-consistently incorporates magnetoelastic coupling together with strain-induced Dzyaloshinskii-Moriya interactions. The influence of mechanical strain on both static and dynamic magnetic configurations is characterised. Results reveal that the interplay between magnetoelastic energy and SIDMI modifies the characteristics of spin-transfer-torque oscillators, enhancing individual device tunability and enabling robust phase locking across oscillator arrays. These findings provide design guidelines for next-generation, mechanically reconfigurable spintronic devices.

***Index Terms*—Micromagnetics, strain, spintronics, magnetoelastics.**

I. SINTRODUCTION

SPINTRONICS and straintronics are envisioned to play important roles in a set of applications, such as high-density data storage, wave computing, neuromorphic computing and related applications in emerging electronics platforms [1-3]. These platforms demand a comprehensive understanding of nonlinear dynamics of spatially inhomogeneous magnetization states.

Strain and the magnetization can be coupled in multiple ways, including magnetoelastic interactions (MEI) via magnetostriction and inverse magnetostriction as well as via strain induced Dzyaloshinskii-Moriya interactions (SIDMI). Such coupling allows controlling static and dynamic magnetization and elastic properties of materials and devices.

Here, we present a study demonstrating how strain can be used to control static and dynamic magnetization states by means of MEI and SIDMI. We show how SIDMI affects static states as well as the dynamics of breathing magnetic skyrmions. We also discuss how MEI can be used to couple spin transfer torque oscillators (STOs).

II. FORMULATION

We consider multi-physics modeling of MEI and SIDMI [1]. We use the Landau-Lifshitz-Gilbert equation (LLGE) for magnetization. The effective magnetic field includes the inverse magnetostriction component to describe MEI as well as SIDIM component. SDIM is a modified interfacial DMI, which is anisotropic with respect to the in-plane directions because of an indirect exchange between neighboring spins mediated by an impurity with a large spin-orbit coupling on heavy metal – ferromagnet interfaces. Elastic statics and dynamics is affected by the magnetization states via the magnetostriction effect as and SIDMI. As a result, hybrid behavior is obtained that can be used to control the functionality of nanomagnetic devices.

The formulation was implemented via a finite element method framework as a part of the FastMag simulator [4]. The micromagnetic component uses first-order nodal tetrahedral or hexahedral elements. The elastic component uses second-order tetrahedral or first-order hexahedral elements. The equations are solved concurrently. At each time step the LLGE and elastic solutions are obtained using implicit second-order time evolution. Their self-consistency is achieved via an iterative process. The approach allows for accounting for a two-way coupling between magnetization and elastic behaviors.

III. STATIC AND DYNAMIC BEHAVIOR

A. Static magnetization states

We start by showing how the magnetization states in a thin film can be controlled by a static strain. Figure 1 presents phase diagrams of magnetic textures that emerge in thin CoFe films as a function of anisotropic in-plane strain, defined by the relation $\varepsilon_{xx} = -2.7\varepsilon_{yy}$, and film thickness d, for the parameter K_e=10, which quantifies the strength of strain-dependent Dzyaloshinskii–Moriya interaction (DMI). The diagrams reveal how the interplay between elastic strain and film thickness influences the stability of various magnetic phases through modulation of interfacial DMI. The system supports a broad range of magnetic textures including ferromagnetic (FM) order at low strain, X-stripe and Y-stripe phases at negative and positive strain respectively, and a prominent central region of coexisting helical and skyrmion states. A distinct out-of-plane magnetized phase appears at high tensile strain and low thickness, while the helical and skyrmion region persists in a narrower strain range. These results highlight the critical role of strain-controlled DMI in tuning magnetic order in CoFe thin films, offering a route to engineer complex spin textures through mechanical means. The insets show representative spin textures for stripe and skyrmion configurations.

B. Breathing skyrmions

Figure 2 illustrates the nonlinear response of a magnetic system by presenting the ratio of the second harmonic to the first harmonic magnitude under varying driving amplitudes and frequencies. Panel (a) demonstrates how this harmonic ratio evolves with increasing strain amplitude (ε_{zz}) for two cases: with and without strain-induced SIDMI, denoted by $\eta = 0.5$ (red) and $\eta = 0$ (blue), respectively. A striking enhancement is observed at a driving frequency of 1.75 GHz (half the system's primary resonance), where the second harmonic magnitude reaches approximately 80% of the first harmonic for a minute strain of just 0.02%. This represents over a 400% increase

compared to the system without SIDMI, highlighting the strong nonlinear behavior.

Panel (b) shows the second-to-first harmonic ratio as a function of driving frequency for a fixed amplitude. The red points (η = 0.5) exhibit significantly stronger second harmonic generation in the low-frequency range, particularly near subharmonic resonances. Even at high frequencies (10–20 GHz), the presence of SIDMI maintains a noticeable nonlinear response, with second harmonic components accounting for about 3–5% of the primary response—still roughly 30 times higher than in the absence of SIDMI, where the second harmonic contribution is nearly negligible (~0.1%).

Insets in both panels provide supporting spectral data and comparative amplitude ratios, reinforcing the role of SIDMI in enhancing harmonic generation in a broad frequency range.

C. Coupled oscillators

Figure 3 shows the spatial distribution of the strain field generated by two spin-torque oscillators (STOs) embedded in a 3 nm-thick ferromagnetic film. The oscillators, with labeled average magnetization vectors $\mathbf{m}_1$ and $\mathbf{m}_2$, are separated by approximately 2 microns. The color map represents the strain component induced by magnetoelastic interactions, with localized patterns centered around each oscillator, indicating the generation of propagating elastic waves. The magnetization dynamics of each STTO acts as a source of elastic waves due to the magnetoelastic coupling. These waves mediate long-range interactions between the oscillators, effectively coupling them over micron-scale distances—well beyond the ~1 μm limit typically imposed by exchange and dipolar (demagnetization) interactions. Importantly, this coupling is bidirectional: while magnetization dynamics emit strain waves (direct magnetostriction), the strain field, in turn, modifies the local magnetic state via the inverse magnetostrictive effect. This mutual feedback enables efficient synchronization or interaction of distant oscillators via the elastic channel. The visualization emphasizes the non-local nature of this coupling mechanism, offering a pathway to design densely packed, elastically interconnected STO arrays without relying on short-range magnetic interactions.

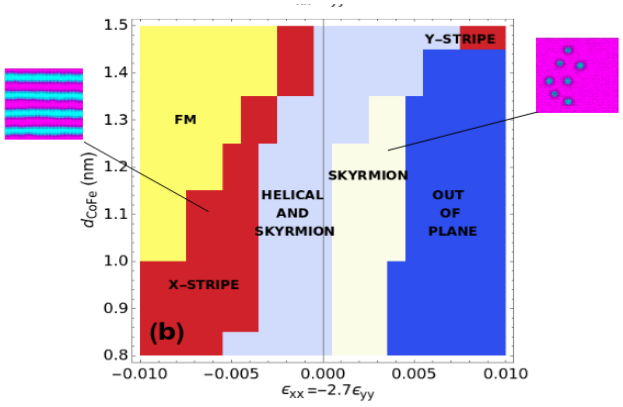

Fig. 1. Phase diagram of static magnetization states controlled by SIDMI.

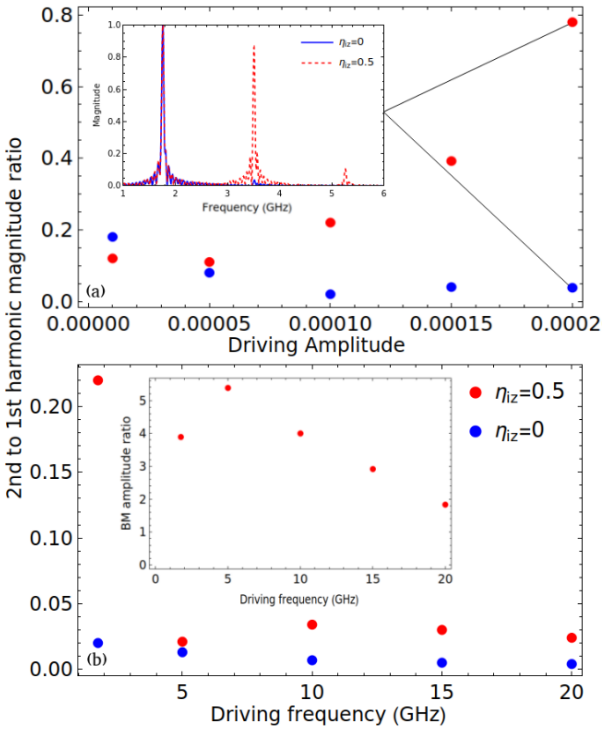

Fig. 2. The ratios between the magnitudes of the n = 2 to n = 1 harmonics as a function of the elastic wave amplitude of (a) 1.75 GHz and (b) 0.01 % of deformations. The inset in Fig. 4(b) shows the ratio of the real-space BM amplitudes for ηiz = 0.5 (with SIDMI) and ηiz = 0(without SIDMI)..

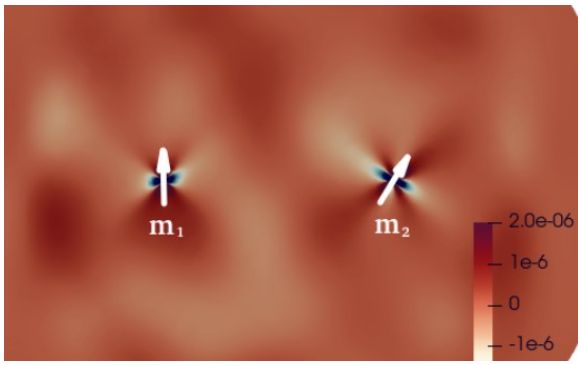

Fig. 3. Synchronization of STOs by means of elastic waves.

REFERENCES

[1] E. Savostin and V. Lomakin, "Giant phonon–skyrmion interaction mediated by strain-induced Dzyaloshinskii–Moriya interaction," *Phys. Rev. B*, vol. 110, p. 064423, 2024.

[2] C. Kittel, "Interaction of spin waves and ultrasonic waves in ferromagnetic crystals," *Phys. Rev.*, vol. 110, pp. 836–841, Apr. 1958.

[3] N. S. Gusev, A. V. Sadovnikov, S. A. Nikitov, M. V. Sapozhnikov, and O. G. Udalov, "Manipulation of the Dzyaloshinskii–Moriya interaction in Co/Pt multilayers with strain," *Phys. Rev. Lett.*, vol. 124, p. 157202, Apr. 2020.

[4] R. Chang, S. Li, M. Lubarda, B. Livshitz, V. Lomakin, "FastMag: Fast micromagnetic simulator for complex magnetic structures," *J. Appl. Phys.*, vol. 109, p. 07D358, 2011.